NIH Public Access
Author Manuscript
Gene Expr Patterns. Author manuscript; available in PMC 2012 January 1.

Published in final edited form as:
Gene Expr Patterns. 2011 ; 11(1-2): 135–143. doi:10.1016/j.gep.2010.10.005.

Unfolded Protein Response (UPR) is activated during normal lens development

Zeynep Firtina and **Melinda K. Duncan***
Department of Biological Sciences, University of Delaware, Newark, DE, USA, 19716

Abstract

The lens of the eye is a transparent structure responsible for focusing light onto the retina. It is composed of two morphologically different cell types, epithelial cells found on the anterior surface and the fiber cells that are continuously formed by the differentiation of epithelial cells at the lens equator. The differentiation of an epithelial precursor cell into a fiber cell is associated with a dramatic increase in membrane protein synthesis. How the terminally differentiating fiber cells cope with the increased demand on the endoplasmic reticulum for this membrane protein synthesis is not known. In the present study, we have found evidence of Unfolded Protein Response (UPR) activation during normal lens development and differentiation in the mouse. The ER-resident chaperones, immunoglobulin heavy chain binding protein (BiP) and protein disulfide isomerase (PDI), were expressed at high levels in the newly forming fiber cells of embryonic lenses. These fiber cells also expressed the UPR-associated molecules; XBP1, ATF6, phospho-PERK and ATF4 during embryogenesis. Moreover, spliced XBP1, cleaved ATF6, and phospho-eIF2 were detected in embryonic mouse lenses suggesting that UPR pathways are active in this tissue. These results propose a role for UPR activation in lens fiber cell differentiation during embryogenesis.

1. Results and Discussion

The lens of the eye is a transparent structure responsible for focusing light onto the retina. It is composed of two morphologically different cell types, epithelial cells and fiber cells, surrounded by a thickened basement membrane called the lens capsule (Danysh and Duncan, 2009; Fukushi and Spiro, 1969). The lens epithelium forms a monolayer of cuboidal cells beneath the anterior capsule. The remainder of the lens is composed of concentric layers of elongated fiber cells that are derived from differentiation of epithelial cells at the lens equator (Bloemendal, 1977; Piatigorsky, 1981). The differentiation of an epithelial precursor cell into a fiber cell is morphologically manifested by an increase in cell length accompanied by a dramatic increase in membrane surface area and membrane elaborations (Bassnett, 2005; Lim et al., 2009). Since the lens is an avascular tissue (Beebe, 2008), the membranes of fiber cells are highly equipped with proteins that aid in establishing communication with neighboring cells. For instance, in some species, more than 50% of the fiber cell plasma membrane is composed of gap junctions (Bassnett et al., 2009; Lo and Harding, 1986). Since these proteins are very different than those found in the epithelial cell precursor (Bassnett et al., 2009), there is a significant increase in the production of

*To whom all the correspondence should be addressed: Melinda K. Duncan, Ph.D., Professor and Graduate Program Director, Department of Biological Sciences, Newark, DE 19716, (302) 831-0533; FAX (302) 831-2281, Duncanm@udel.edu.

Publisher's Disclaimer: This is a PDF file of an unedited manuscript that has been accepted for publication. As a service to our customers we are providing this early version of the manuscript. The manuscript will undergo copyediting, typesetting, and review of the resulting proof before it is published in its final citable form. Please note that during the production process errors may be discovered which could affect the content, and all legal disclaimers that apply to the journal pertain.

NIH-PA Author Manuscript
NIH-PA Author Manuscript
NIH-PA Author Manuscript

NIH-PA Author Manuscript

NIH-PA Author Manuscript

NIH-PA Author Manuscript

membrane proteins during fiber cell differentiation. It is not known how terminally differentiating fiber cells cope with the increased demand of this high level of membrane protein synthesis.

Normal differentiation and development of secretory cell types, such as plasma cells and pancreatic beta cells, leads to a high protein load in the ER/Golgi secretory pathway. Under this developmental ER stress, these cells rely on the activation of UPR, a stress-induced signaling pathway emanating from the ER, to enhance their protein folding capacity (Iwakoshi et al., 2003; Zhang et al., 2002). UPR pathways are activated upon unfolded protein accumulation in the ER and try to relieve the stress by 1) upregulating the ER folding capacity through increasing the levels of ER-resident molecular chaperones and expansion of the ER, 2) reducing the demand on the ER through attenuation of protein synthesis, and 3) increasing the clearance of unfolded proteins from the ER through upregulation of ER associated degradation (ERAD). However if these mechanisms cannot relieve the stress, the UPR pathway activates apoptosis (Kaufman, 1999; Ron and Walter, 2007; Rutkowski and Kaufman, 2004).

It has been previously proposed that UPR can be induced in lens epithelial cells by osmotic and oxidative insults and this UPR activation could influence cataractogenesis (Ikesugi et al., 2006; Mulhern et al., 2006). We have previously reported that UPR is highly activated in the lenses of mice expressing misfolded collagen chains and this activation is associated with diverse lens pathologies (Firtina et al., 2009). While conducting these studies, we also noted that these pathways were activated at moderate levels during normal lens development as well (Firtina et al., 2009). Here we delineate this physiological UPR activation during lens development.

1.1. The expression of ER chaperones in embryonic and adult lens

During differentiation, newly forming fiber cells elongate bidirectionally and move deeper into the lens as their basal ends migrate along the posterior capsule and their apical ends migrate along the apical surface of the anterior lens epithelium (Kuszak et al., 2004; Rao, 2008). Endoplasmic reticulum and nuclei are present in the newly forming fiber cells; however as fiber cells mature, they undergo denucleation and degrade their cytoplasmic organelles as a feature of terminal differentiation. Thus, the center of the adult lens is composed of mature fiber cells that are devoid of nuclei and any membrane-bound organelles (Bassnett, 1995; Bassnett, 2009). In this study, we followed the expression of two ER-resident chaperones, immunoglobulin heavy chain binding protein (BiP) and protein disulfide isomerase (PDI), during normal lens development. By embryonic day 11.5, cells of the posterior lens vesicle exit the cell cycle and elongate to form primary fiber cells which eventually fill the lens vesicle and make apical-apical contacts with the lens epithelium. By immunostaining, we showed that both ER chaperones are expressed in lens epithelium and fiber cells at E12.5. (Figure 1A, top panels). Later, the expression of both ER-chaperones in lens fiber cells becomes relatively higher at the transition zone (Figure 1A, middle and bottom panels). Right before birth at E18.5, BiP and PDI expressions are still high in the lens epithelium and newly forming lens fiber cells, while only diffuse staining is seen in central lens fiber cells that are in the process of losing their nuclei and organelles. (Figure 1B, top panels). In 3 month old lenses, the expression of BiP and PDI almost disappears in early fiber cells, whereas epithelial cells are strongly stained. Interestingly, both BiP and PDI expression are also associated with nuclei that are being degraded during fiber cell maturation. This could suggest the aggregation of endoplasmic reticulum against the nuclear envelope during degradation (Figure 1B, middle panels). The bottom panels of Figure 1B show higher magnifications highlighting the two patterns of PDI staining observed in maturing fiber cells: perinuclear staining in lens fiber cells that are preparing to undergo degradation of nuclei and organelles and a more concentrated dot-like staining at the tips of

NIH-PA Author Manuscript

NIH-PA Author Manuscript

NIH-PA Author Manuscript

the degrading nuclei. Western blotting analysis confirmed that BiP levels are high in the lens during embryogenesis (Figure 2). The relatively low amounts of BiP detected by western blotting in postnatal lenses in comparison to total actin levels likely reflects both the relatively low percentage of nucleated lens fiber cells containing ER present in adult lenses and the relatively lower levels of expression in nucleated fibers detected by immunofluorescence (Figure 1B). Relative PDI levels as measured by western blot did not change dramatically in the lens during development but did decrease by about one half of those detected in E 14.5 lens. Overall, these data suggested that newly forming fiber cells of the embryonic lens are enriched in ER. We then proceeded to determine if the increased expression of ER chaperones in embryonic lens fibers is correlated with activation of UPR pathways in lens fiber cells.

1.2. The activation of the IRE1/XBP1 pathway in embryonic and adult lenses

The UPR pathway that has been conserved from yeast to mammals is transduced by Inositol-requiring enzyme 1 (IRE1), an atypical type I transmembrane protein consisting of an ER luminal dimerization domain, as well as cytosolic kinase and endoribonuclease domains (Patil and Walter, 2001; Shamu and Walter, 1996). Activated IRE1 removes a 26-base intron from the *Xbp1* mRNA, introducing a frameshift and an alternative C-terminus to create a potent transcription factor (Back et al., 2005; Lee et al., 2002). We performed immunostaining in mouse lenses using an XBP1 antibody that detects both XBP1(S) and XBP1 (U) which are produced from spliced and unspliced *Xbp1* mRNAs, respectively. During the initial stages of mouse eye formation (E9.5 to E11.5), there is little to no XBP1 immunoreactivity detected in the lens (Figure 3A, top panels). However, by E12.5, XBP1 immunoreactivity becomes detectable in primary fiber cells, localized mostly at the apical and basal tips. At this age, there is little XBP1 expression in the lens epithelium. (Figure 3A, bottom panels). The expression of XBP1 in lens fiber cells is maintained at E13.5 (Figure 3B, top panels). However by E14.5, XBP1 levels downregulate in lens fiber cells while epithelial XBP1 expression increases (Figure 3B, bottom panels). At E17.5, along with the cornea, the lens epithelium shows high XBP1 expression (Figure 3C, top panels) while in lens fiber cells, XBP1 expression is lower and only observed in peripheral fiber cells (Figure 3B, bottom panels). In adult lenses, epithelial XBP1 expression remain elevated (Figure 3C, top panels) while XBP1 expression in lens fibers is now only confined to a small area consisting of a few newly formed lens fiber cells (Figure 3C, bottom panels).

To determine if IRE1-mediated splicing of *Xbp1* mRNA occurs in the lens during development, we performed RT-PCR analysis using primers designed to differentiate between spliced and unspliced forms of *Xbp1* mRNA. Figure 4A demonstrates that there is a basal level of *Xbp1* splicing throughout lens development (Figure 4A). To quantify the amount of *Xbp1* splicing, we performed real-time RT-PCR analysis as described in Back et. al (Back et al., 2005). Two set of primers were used to amplify total (both spliced and unspliced) or specifically spliced forms of *Xbp1* transcripts. Our results suggest that the spliced form of Xbp1 transcript is produced in the lens throughout development (Figure 4B) and represents about 17% of total Xbp1 transcripts at E14.5 and about 32% of total Xbp1 transcripts at 2.5 months (Figure 4C). However, when the protein products of these transcripts were analyzed by western blotting (Figure 5), embryonic lenses had higher levels of the protein generated from the spliced *Xbp1* mRNA (54 kDa) whereas postnatal lenses had higher relative levels of the protein generated from unspliced *Xbp1* mRNA (33 kDa). It can be speculated that XBP1(U) protein functions to downregulate XBP1(S) in postnatal lenses, consistent with the proposed function of XBP1(U) as a negative regulator of XBP1(S) through direct binding and directing it for proteasomal degradation (Yoshida et al., 2006). However other functions of this protein in mammals are still unclear and its role in normal lens development and differentiation needs to be investigated. Prolonged or strong

NIH-PA Author Manuscript

NIH-PA Author Manuscript

NIH-PA Author Manuscript

activation of the IRE1 pathway is linked to activation of the proapoptotic c-jun N-terminal kinase (JNK) pathway and/or activation of caspase 12 and can lead to apoptosis (Szegezdi et al., 2003; Urano et al., 2000). Thus this pathway might be tightly regulated during lens development to prevent the induction of apoptosis. XBP(S) is a basic leucine zipper (bZIP) transcription factor that can regulate ER chaperones, ER-associated degradation (ERAD), and ER biogenesis (Friedlander et al., 2000; Lee et al., 2003; Sriburi et al., 2004). Recently, XBP1(S) has been identified as the transcription factor that is specifically required for the terminal differentiation of B lymphocytes into plasma cells (Iwakoshi et al., 2003; Reimold et al., 2001). When introduced into a B-cell line, XBP1(S) can initiate plasma cell differentiation and is sufficient to induce the proliferation of ER, Golgi, mitochondria and lysosomes (Shaffer et al., 2004). Since differentiation involves synthesis of high amounts of membrane proteins, XBP1(S)'s function in the lens might also involve upregulating ER folding capacity through induction of ER chaperones, ER-folding enzymes and ER biogenesis in differentiating fiber cells.

1.3. The activation of the ATF6 pathway in embryonic and adult lens

Another sensor activated in mammalian UPR is activating transcription factor 6 (ATF6). There are two ATF6 genes in mammals, ATF6 and ATF6 that appear to be regulated by the same mechanism. Upon ER stress, ATF6 proteins progress to the Golgi where they are cleaved by S1P and S2P proteases; liberating their cytosolic domain as soluble transcription factors (Haze et al., 1999; Shen et al., 2002; Ye et al., 2000). We used an ATF6 / antibody that detects both the intact and cleaved (nuclear) forms. At E11.5, there is a low level of ATF6 / expression detected in the retina and in posterior lens vesicle cells (Figure 6A, top panels). However once the lens vesicle fills with elongating fiber cells to form the early lens at E12.5, ATF6 / is highly expressed by the nuclei of lens fiber cells (Figure 6A, bottom panels). At E14.5, ATF6 / expression is maintained in the fiber cell nuclei (Figure 6B, bottom panels) while lens epithelium is also diffusely stained. Right before birth, at E18.5, the expression of ATF6 / is detected highest at the transition zone where youngest lens fiber cells are forming (Figure 6C). In 3 months old adult lenses, ATF6 / expression is still detectable in peripheral young lens fiber cells and in the lens epithelium although the levels appear reduced (Figure 6D).

Since ATF6 is cleaved into a shorter protein upon activation, we performed western blotting to assess if ATF6 / cleavage is induced during normal lens development. We have demonstrated that both in embryonic and newborn lenses, pro-ATF6 / is cleaved into a ~50 kDa protein suggesting that the ATF6 pathway is active both pre and postnatally (Figure 7). The cleaved forms of ATF6, termed ATF6 (N) are basic leucine zipper (bZIP) transcription factors that bind to cis-acting promoter sequences called ER-stress response elements (ERSE) to induce target genes which are mostly ER-resident molecular chaperones and folding enzymes (Thuerauf et al., 2004;Wu et al., 2007). Thus, the ATF6 pathway is believed to be predominately required for the adaptive signaling needed to induce the full induction of ER-folding capacity. ATF6 can also induce transcription of ERAD components through heterodimerization with XBP(S) (Yamamoto et al., 2007). Moreover, Bommiasamy et. al recently showed that forced expression of ATF6 is capable of driving ER expansion in the absence of XBP1(S) (Bommiasamy et al., 2009). This suggests that ATF6 and XBP1(S) can both collectively and distinctly regulate ER folding capacity through the upregulation of ER-folding machinery and ER biogenesis. Thus, these two proteins may cooperate to drive the expansion of the protein folding apparatus by upregulating the expression of ER-chaperones, ER-folding enzymes and ERAD components in differentiating fiber cells that need to synthesize high amounts of membrane proteins.

NIH-PA Author Manuscript

NIH-PA Author Manuscript

NIH-PA Author Manuscript

1.4. The activation of the PERK-peIF2 pathway in embryonic and adult lenses

The third UPR pathway is mediated by PKR-like ER kinase (PERK), an ER transmembrane protein, whose luminal domain senses ER stress, and cytoplasmic domain directly phosphorylates eukaryotic initiation factor 2 (eIF2) on serine 51 leading to its inactivation. This results in the inhibition of translational initiation for most cellular mRNAs and decreased folding demand on the ER (Brostrom and Brostrom, 1998; Harding et al., 2000b). To be activated, PERK undergoes oligomerization and subsequent autophosphorylation at multiple sites. We used an antibody specific to a form of PERK phosphorylated at Thr980 to detect active PERK expression in the lens. p-PERK immunoreactivity is first observed at E12.5 and is localized to the apical tips of lens fiber cells (Figure 8A, bottom panels). In later embryos, p-PERK expression is maintained at high levels predominately at the apical tips of the newly forming lens fiber cells while it is reduced in central fiber cells (Figure 8B). By 18.5, p-PERK expression is now mostly confined to the newly forming lens fiber cell apical tips (Figure 8C). It has been demonstrated previously that elements of the endoplasmic reticulum are particularly concentrated at the posterior and apical tips of elongating lens fiber cells (Bassnett, 1995). However it has also been argued that individual ER-resident protein expression patterns might vary due to functional compartmentalization of ER proteins in different types of ER (Bassnett, 1995). To date, there has not been a study showing the localization of different types of ER (e.g., smooth vs. rough) in the lens fiber cells. The specific localization of p-PERK at the apical tips of lens fiber cells might suggest that rough endoplasmic reticulum is enhanced at these tips. It is known that, in pancreas, the regulation of translation rate by PERK is necessary to adjust the rate of insulin synthesis according to the blood glucose levels (Scheuner et al., 2001). In the lens, since epithelial to fiber transformation involves a drastic increase in membrane protein production, PERK might be necessary to prevent the ER-folding machinery from being overwhelmed during this transformation. Alternatively, PERK might also have a more specific role in the lens. It has recently been shown that in mammary gland, PERK promotes lipid synthesis by promoting SREBP1 activation via depletion of its inhibitory protein, Insig1. Since Insig1 is a short-lived protein, eIF2 -mediated translational inhibition quickly depletes this protein. In the absence of Insig1, SREBP1 can translocate to the Golgi where it is cleaved by S1/S2P proteases to produce a transcription factor that can induce lipogenic enzymes (Bobrovnikova-Marjon et al., 2008). It can be speculated that PERK functions similarly in the lens. Lens plasma membranes are extremely rich in cholesterol and phospholipid (Borchman and Yappert, 2010). The activation of the PERK at the apical tips of lens fiber cells might suggest that PERK regulates the production of membrane lipids that are needed to be integrated into the rapidly elongating membrane tips of these fiber cells. However, further research is needed to identify the significance of PERK-mediated translational control in lens physiology.

Interestingly, in three month old lenses, p-PERK expression is no longer seen at the apical tips of lens fiber cells. Instead, p-PERK expression becomes associated with the degrading nuclei in mature fiber cells. The association of p-PERK expression with these nuclei might suggest that p-PERK is involved in this degradation process. It is known that the disappearance of nuclei, endoplasmic reticulum and mitochondria coincides during terminal differentiation suggesting that this is a coordinated process (Bassnett, 1995). It can be speculated that PERK signaling might be involved in coordinating the degradation of organelles with denucleation. Interestingly, our previous data have suggested that the persistent activation of UPR in central fiber cells results in the retention of nuclei and organelles (Firtina et al., 2009). Thus, even though PERK signaling could be needed to regulate this process, eventually, the shutdown of the UPR in central fiber cells might be required for proper denucleation.

NIH-PA Author Manuscript

NIH-PA Author Manuscript

NIH-PA Author Manuscript

We also analyzed whether the downstream target of active PERK, e-IF2 is phosphorylated during lens development. Western blotting demonstrated that phosphorylation of e-IF2 starts to increase around E14.5 and remains elevated at E15.5 and E16.5; however its levels downregulate postnatally suggesting that this pathway is mostly active during embryogenesis (Figure 9A). Since prolonged or strong activation of the PERK pathway is linked to apoptosis, this pathway might be selectively suppressed or kept at low activation levels during lens development to prevent the induction of apoptosis. The deleterious effect of the PERK pathway has been shown to involve upregulation of CHOP and its pro apoptotic targets in other systems. Consistently, we did not detect any CHOP expression during normal lens development (our unpublished observation).

PERK-mediated phosphorylation of eIF2 also results in the enhanced translation of ATF4, a b-ZIP transcription factor of the cyclic-AMP response element-binding (CREB) family (Harding et al., 2000a; Harding et al., 2000b). Immunostaining and western blotting analysis of ATF4 suggests that ATF4 levels increase in lens fiber cells at E12.5 (Figure 9B) and stay up through E14.5; however downregulate after that (Figure 9A,B). Previously, ATF4 null lenses have been shown to undergo p53-mediated cell death demonstrating the importance of ATF4 in lens homeostasis (Tanaka et al., 1998). Thus, PERK mediated eIF2 phosphorylation might be required to induce ATF4 expression in the lens. ATF4 is known to regulate genes involved in the synthesis and transport of amino acids. ATF4 also protects cells against oxidative stress, by modulating a number of genes involved in mitochondrial function (e.g., mitochondrial stress-HSP70 chaperone), redox chemistry (e.g., NADH-cytochrome B5 reductase homologue), and reduced glutathione (GSH) metabolism (e.g., system X_C^- light chain (xCT)) (Harding et al., 2003; Lewerenz and Maher, 2009). Besides ER stress, hypoxia also can activate PERK and induce ATF4 translation. Cells with compromised PERK-eIF2 -ATF4 signaling have shown to be more sensitive to hypoxic stress in vitro indicating that the PERK-eIF2 -ATF4 pathway confers a survival advantage under hypoxia (Koumenis et al., 2002). Interestingly, the avascular lens exists in a hypoxic environment (Beebe, 2008; Shui and Beebe, 2008) and this hypoxic environment is required for lens transparency since increased exposure to oxygen has been shown to be a risk factor for age-related cataract (Giblin et al., 2009; McNulty et al., 2004; Shui et al., 2009). Thus, the role of ATF4 in the lens might involve maintaining lens cell survival under hypoxic conditions. Alternatively, ATF4 might be involved in a function unrelated to stress in the lens. ATF4 regulates osteoblast differentiation through binding to osteoblast-specific element 1(OSE1), found in the osteocalcin gene (Yang and Karsenty, 2004). Similarly, in chondrocytes, ATF4 regulates proliferation and differentiation through transcriptional activation of Indian Hedgehog (Ihh) (Wang et al., 2009). Thus, ATF4 in the lens might function to upregulate genes that encode proteins involved in lens differentiation. Nevertheless, further research is needed to determine the role of ATF4 in lens development and physiology.

Previously we reported that UPR is highly activated in lenses expressing misfolded collagen chains and correlated this activation with diverse lens pathologies resulting in cataract (Firtina et al., 2009). In the present study, we show that the expression/activation of a variety of UPR markers is developmentally regulated in the lens suggesting that the UPR pathway is activated, albeit at a relatively low level, during normal lens differentiation. The functional consequences of this activation are currently unknown but should be a topic of future research.

NIH-PA Author Manuscript
NIH-PA Author Manuscript
NIH-PA Author Manuscript

2. Experimental Procedures

Animals

FVB/N-Har breeders were obtained from Harlan Laboratories and all mice in this study were bred and maintained in the University of Delaware Transgenic Animal Facility.

Embryos used in the study are staged by designating the day that the vaginal plug was observed in the dam as 0.5 days post coitum (dpc). Postnatal mice were staged by designated the day of birth as 0 day postnatal.

Immunofluorescence

All immunofluorescence experiments were performed as previously described (Reed et al., 2001). Briefly, lenses were isolated and immediately embedded in Optimum Cutting Temperature media (OCT, Tissue Tek, Torrance California). Sixteen μm thick sections were cut with a cryostat and mounted on ColorFrost plus slides (Fisher Scientific, Hampton, New Hampshire). For staining with most antibodies, sections were fixed in ice cold 1:1 acetone–methanol for 20 min at −20 °C, blocked in 1% BSA for 1 h at room temperature, followed by the incubation with the appropriate dilution of primary antibody (see Table 1) for an additional hour. Sections were then washed two times for 10-minutes each and detected with the appropriate AlexaFluor 568 labeled secondary antibody (Molecular Probes, Eugene Oregon) prepared in 1% BSA containing 1:2000 diluted Draq-5 as the nuclear stain (Biostatus Limited, Leicestershire, United Kingdom). Slides were then visualized using a Zeiss LSM 510 confocal microscope (Carl Zeiss Inc, Göttingen, Germany). Identical conditions were used to do the imaging of each antibody at different ages to ensure the validity of comparisons.

Phospho-PERK staining was performed by the standard method above, however, the primary antibody was instead incubated overnight at 4 °C.

RNA Preparation and conventional RT-PCR—Total RNA from lenses was extracted using the SV Total RNA Isolation Kit (Promega, Madison, Wisconsin). For RT-PCR, 20 ng of total RNAs were used for each sample. The primers used are Xbp1 Fwd 5′ GAA CCA GGA GTT AAG AAC ACG 3′and Xbp1 Rev 5′ AGG CAA CAG TGT CAG AGT CC 3′ for Xbp1 splicing. The identities of the spliced and unspliced XPB-1 bands were confirmed by sequence analysis.

Synthesis of cDNA and Real-time RT-PCR—300ng of total RNAs were used to synthesize cDNA using RT^2 First Strand Kit (SABiosciences, Frederick, MD) for each age examined. Briefly, each RNA sample was incubated in gDNA elimination buffer (provided in the kit) at 42°C for 5 minutes and then chilled on ice immediately for at least one minute. For cDNA synthesis reactions, the RT Cocktail was prepared using the RT buffer, primer mix and enzyme mix provided in the kit. 10 l of this RT Cocktail was added on 10 l of RNA in gDNA elimination buffer and this mixture was incubated at 42°C for 15 minutes. The reaction was then stopped by heating at 95°C for 5 minutes and diluted by adding 91 l of H_2O. 1 l of this cDNA was used to perform real-time RT-PCR using the RT^2 SYBR Green qPCR Master Mix (SABiosciences, Frederick, MD).

Western Blotting—For each age point examined, several wild type FVB/N lenses were isolated and collected in a test tube on dry ice. These lenses were then immediately homogenized with 0.1 ml of ice-cold lysis buffer (50mM Tris-HCl, pH 8.0, 150 mM NaCl, 1% NP-40, 0.5% Na-deoxycholate, 0.1% SDS) supplemented with Halt Protease and Phosphatase Inhibitor Cocktail (Thermo Scientific, Rockford, IL). The insoluble material

NIH-PA Author Manuscript

NIH-PA Author Manuscript

NIH-PA Author Manuscript

was removed by centrifugation at 12,000g for 30 minutes. Final protein concentrations were determined using a Bio-Rad protein assay kit (Bio-Rad, Hercules, CA) according to the manufacturer's specifications. Forty micrograms of total protein were resolved by SDS-polyacrylamide gel and transferred onto supported nitrocellulose membranes (Bio-Rad, Hercules, CA). The protein blots were blocked with SuperBlock T20 Blocking Buffer (Thermo Scientific, Rockford, IL) overnight at 4°C and incubated with the primary antibody in the same blocking buffer for 2 hours. After incubation with secondary antibodies conjugated with horseradish peroxidase (Calbiochem, San Diego, CA) for 1 hour at room temperature, the signals were detected using an enhanced chemiluminescence detection kit. (Amersham Biosciences, Piscataway, NY). All western blot experiments were repeated at least three times. The intensity of the signal for molecules of interest was quantified using Photoshop Histogram Analysis.

Note that the same antibodies were used in western blotting experiments as described in Firtina et. al (Firtina et al., 2009). However, in the present study the exposure times of the membranes were considerably increased compared to our prior study due to the relatively low abundance of UPR molecules in wild type lenses.

Acknowledgments

We thank Amal Ali Aldossary for technical assistance with ATF4 immunostainings. This work was supported by a grant from National Eye Institute to MKD (EY015279). INBRE program grant P20 RR16472 supported the University of Delaware Core Imaging facility. ZF is a recipient of a Sigma Xi-NAS grant in aid.

References

Back SH, Schroder M, Lee K, Zhang K, Kaufman RJ. ER stress signaling by regulated splicing: IRE1/HAC1/XBP1. Methods 2005;35:395–416. [PubMed: 15804613]

Bassnett S. The fate of the Golgi apparatus and the endoplasmic reticulum during lens fiber cell differentiation. Invest Ophthalmol Vis Sci 1995;36:1793–803. [PubMed: 7635654]

Bassnett S. Three-dimensional reconstruction of cells in the living lens: the relationship between cell length and volume. Exp Eye Res 2005;81:716–23. [PubMed: 15963502]

Bassnett S. On the mechanism of organelle degradation in the vertebrate lens. Exp Eye Res 2009;88:133–9. [PubMed: 18840431]

Bassnett S, Wilmarth PA, David LL. The membrane proteome of the mouse lens fiber cell. Mol Vis 2009;15:2448–63. [PubMed: 19956408]

Beebe DC. Maintaining transparency: A review of the developmental physiology and pathophysiology of two avascular tissues. Seminars in Cell & Developmental Biology 2008;19:125–133. [PubMed: 17920963]

Bloemendal H. The vertebrate eye lens. Science 1977;197:127–38. [PubMed: 877544]

Bobrovnikova-Marjon E, Hatzivassiliou G, Grigoriadou C, Romero M, Cavener DR, Thompson CB, Diehl JA. PERK-dependent regulation of lipogenesis during mouse mammary gland development and adipocyte differentiation. Proc Natl Acad Sci U S A 2008;105:16314–9. [PubMed: 18852460]

Bommiasamy H, Back SH, Fagone P, Lee K, Meshinchi S, Vink E, Sriburi R, Frank M, Jackowski S, Kaufman RJ, et al. ATF6alpha induces XBP1-independent expansion of the endoplasmic reticulum. J Cell Sci 2009;122:1626–36. [PubMed: 19420237]

Borchman D, Yappert MC. Lipids and the ocular lens. J Lipid Res. 2010 jlr.R004119.

Brostrom CO, Brostrom MA. Regulation of translational initiation during cellular responses to stress. Prog Nucleic Acid Res Mol Biol 1998;58:79–125. [PubMed: 9308364]

Danysh BP, Duncan MK. The lens capsule. Exp Eye Res 2009;88:151–64. [PubMed: 18773892]

Firtina Z, Danysh BP, Bai X, Gould DB, Kobayashi T, Duncan MK. Abnormal expression of collagen IV in lens activates unfolded protein response resulting in cataract. J Biol Chem 2009;284:35872–84. [PubMed: 19858219]

NIH-PA Author Manuscript

NIH-PA Author Manuscript

NIH-PA Author Manuscript

Friedlander R, Jarosch E, Urban J, Volkwein C, Sommer T. A regulatory link between ER-associated protein degradation and the unfolded-protein response. Nat Cell Biol 2000;2:379–84. [PubMed: 10878801]

Fukushi S, Spiro RG. The lens capsule. Sugar and amino acid composition. J Biol Chem 1969;244:2041–8. [PubMed: 5781998]

Giblin FJ, Quiram PA, Leverenz VR, Baker RM, Dang L, Trese MT. Enzyme-induced posterior vitreous detachment in the rat produces increased lens nuclear pO2 levels. Experimental Eye Research 2009;88:286–292. [PubMed: 18835558]

Harding HP, Novoa I, Zhang Y, Zeng H, Wek R, Schapira M, Ron D. Regulated translation initiation controls stress-induced gene expression in mammalian cells. Mol Cell 2000a;6:1099–108. [PubMed: 11106749]

Harding HP, Zhang Y, Bertolotti A, Zeng H, Ron D. Perk is essential for translational regulation and cell survival during the unfolded protein response. Mol Cell 2000b;5:897–904. [PubMed: 10882126]

Harding HP, Zhang Y, Zeng H, Novoa I, Lu PD, Calfon M, Sadri N, Yun C, Popko B, Paules R, et al. An integrated stress response regulates amino acid metabolism and resistance to oxidative stress. Mol Cell 2003;11:619–33. [PubMed: 12667446]

Haze K, Yoshida H, Yanagi H, Yura T, Mori K. Mammalian transcription factor ATF6 is synthesized as a transmembrane protein and activated by proteolysis in response to endoplasmic reticulum stress. Mol Biol Cell 1999;10:3787–99. [PubMed: 10564271]

Ikesugi K, Yamamoto R, Mulhern ML, Shinohara T. Role of the unfolded protein response (UPR) in cataract formation. Exp Eye Res 2006;83:508–16. [PubMed: 16643900]

Iwakoshi NN, Lee AH, Vallabhajosyula P, Otipoby KL, Rajewsky K, Glimcher LH. Plasma cell differentiation and the unfolded protein response intersect at the transcription factor XBP-1. Nat Immunol 2003;4:321–9. [PubMed: 12612580]

Kaufman RJ. Stress signaling from the lumen of the endoplasmic reticulum: coordination of gene transcriptional and translational controls. Genes Dev 1999;13:1211–33. [PubMed: 10346810]

Koumenis C, Naczki C, Koritzinsky M, Rastani S, Diehl A, Sonenberg N, Koromilas A, Wouters BG. Regulation of protein synthesis by hypoxia via activation of the endoplasmic reticulum kinase PERK and phosphorylation of the translation initiation factor eIF2alpha. Mol Cell Biol 2002;22:7405–16. [PubMed: 12370288]

Kuszak JR, Zoltoski RK, Tiedemann CE. Development of lens sutures. Int J Dev Biol 2004;48:889–902. [PubMed: 15558480]

Lee AH, Iwakoshi NN, Glimcher LH. XBP-1 regulates a subset of endoplasmic reticulum resident chaperone genes in the unfolded protein response. Mol Cell Biol 2003;23:7448–59. [PubMed: 14559994]

Lee K, Tirasophon W, Shen X, Michalak M, Prywes R, Okada T, Yoshida H, Mori K, Kaufman RJ. IRE1-mediated unconventional mRNA splicing and S2P-mediated ATF6 cleavage merge to regulate XBP1 in signaling the unfolded protein response. Genes Dev 2002;16:452–66. [PubMed: 11850408]

Lewerenz J, Maher P. Basal levels of eIF2alpha phosphorylation determine cellular antioxidant status by regulating ATF4 and xCT expression. J Biol Chem 2009;284:1106–15. [PubMed: 19017641]

Lim JC, Walker KL, Sherwin T, Schey KL, Donaldson PJ. Confocal microscopy reveals zones of membrane remodeling in the outer cortex of the human lens. Invest Ophthalmol Vis Sci 2009;50:4304–10. [PubMed: 19357350]

Lo WK, Harding CV. Structure and distribution of gap junctions in lens epithelium and fiber cells. Cell Tissue Res 1986;244:253–63. [PubMed: 3487382]

McNulty R, Wang H, Mathias RT, Ortwerth BJ, Truscott RJW, Bassnett S. Regulation of tissue oxygen levels in the mammalian lens. The Journal of Physiology 2004;559:883–898. [PubMed: 15272034]

Mulhern ML, Madson CJ, Danford A, Ikesugi K, Kador PF, Shinohara T. The unfolded protein response in lens epithelial cells from galactosemic rat lenses. Invest Ophthalmol Vis Sci 2006;47:3951–9. [PubMed: 16936110]

NIH-PA Author Manuscript

NIH-PA Author Manuscript

NIH-PA Author Manuscript

Patil C, Walter P. Intracellular signaling from the endoplasmic reticulum to the nucleus: the unfolded protein response in yeast and mammals. Curr Opin Cell Biol 2001;13:349–55. [PubMed: 11343907]

Piatigorsky J. Lens Differentiation in Vertebrates. A Review of Cellular and Molecular Features. Differentiation 1981;19:134–153. [PubMed: 7030840]

Rao PV. The pulling, pushing and fusing of lens fibers: a role for Rho GTPases. Cell Adh Migr 2008;2:170–3. [PubMed: 19262112]

Reimold AM, Iwakoshi NN, Manis J, Vallabhajosyula P, Szomolanyi-Tsuda E, Gravallese EM, Friend D, Grusby MJ, Alt F, Glimcher LH. Plasma cell differentiation requires the transcription factor XBP-1. Nature 2001;412:300–7. [PubMed: 11460154]

Ron D, Walter P. Signal integration in the endoplasmic reticulum unfolded protein response. Nat Rev Mol Cell Biol 2007;8:519–529. [PubMed: 17565364]

Rutkowski DT, Kaufman RJ. A trip to the ER: coping with stress. Trends Cell Biol 2004;14:20–8. [PubMed: 14729177]

Scheuner D, Song B, McEwen E, Liu C, Laybutt R, Gillespie P, Saunders T, Bonner-Weir S, Kaufman RJ. Translational control is required for the unfolded protein response and in vivo glucose homeostasis. Mol Cell 2001;7:1165–76. [PubMed: 11430820]

Shaffer AL, Shapiro-Shelef M, Iwakoshi NN, Lee AH, Qian SB, Zhao H, Yu X, Yang L, Tan BK, Rosenwald A, et al. XBP1, downstream of Blimp-1, expands the secretory apparatus and other organelles, and increases protein synthesis in plasma cell differentiation. Immunity 2004;21:81–93. [PubMed: 15345222]

Shamu CE, Walter P. Oligomerization and phosphorylation of the Ire1p kinase during intracellular signaling from the endoplasmic reticulum to the nucleus. EMBO J 1996;15:3028–39. [PubMed: 8670804]

Shen J, Chen X, Hendershot L, Prywes R. ER stress regulation of ATF6 localization by dissociation of BiP/GRP78 binding and unmasking of Golgi localization signals. Dev Cell 2002;3:99–111. [PubMed: 12110171]

Shui Y-B, Beebe DC. Age-Dependent Control of Lens Growth by Hypoxia. Invest Ophthalmol Vis Sci 2008;49:1023–1029. [PubMed: 18326726]

Shui YB, Holekamp NM, Kramer BC, Crowley JR, Wilkins MA, Chu F, Malone PE, Mangers SJ, Hou JH, Siegfried CJ, et al. The Gel State of the Vitreous and Ascorbate-Dependent Oxygen Consumption: Relationship to the Etiology of Nuclear Cataracts. Arch Ophthalmol 2009;127:475–482. [PubMed: 19365028]

Sriburi R, Jackowski S, Mori K, Brewer JW. XBP1: a link between the unfolded protein response, lipid biosynthesis, and biogenesis of the endoplasmic reticulum. J Cell Biol 2004;167:35–41. [PubMed: 15466483]

Szegezdi E, Fitzgerald U, Samali A. Caspase-12 and ER-stress-mediated apoptosis: the story so far. Ann N Y Acad Sci 2003;1010:186–94. [PubMed: 15033718]

Tanaka T, Tsujimura T, Takeda K, Sugihara A, Maekawa A, Terada N, Yoshida N, Akira S. Targeted disruption of ATF4 discloses its essential role in the formation of eye lens fibres. Genes Cells 1998;3:801–10. [PubMed: 10096021]

Thuerauf DJ, Morrison L, Glembotski CC. Opposing roles for ATF6alpha and ATF6beta in endoplasmic reticulum stress response gene induction. J Biol Chem 2004;279:21078–21084. [PubMed: 14973138]

Urano F, Wang X, Bertolotti A, Zhang Y, Chung P, Harding HP, Ron D. Coupling of stress in the ER to activation of JNK protein kinases by transmembrane protein kinase IRE1. Science 2000;287:664–666. [PubMed: 10650002]

Wang W, Lian N, Li L, Moss HE, Perrien DS, Elefteriou F, Yang X. Atf4 regulates chondrocyte proliferation and differentiation during endochondral ossification by activating Ihh transcription. Development 2009;136:4143–53. [PubMed: 19906842]

Wu J, Rutkowski DT, Dubois M, Swathirajan J, Saunders T, Wang J, Song B, Yau GD, Kaufman RJ. ATF6alpha optimizes long-term endoplasmic reticulum function to protect cells from chronic stress. Dev Cell 2007;13:351–64. [PubMed: 17765679]

NIH-PA Author Manuscript

NIH-PA Author Manuscript

NIH-PA Author Manuscript

Yamamoto K, Sato T, Matsui T, Sato M, Okada T, Yoshida H, Harada A, Mori K. Transcriptional induction of mammalian ER quality control proteins is mediated by single or combined action of ATF6alpha and XBP1. Dev Cell 2007;13:365–76. [PubMed: 17765680]

Yang X, Karsenty G. ATF4, the osteoblast accumulation of which is determined post-translationally, can induce osteoblast-specific gene expression in non-osteoblastic cells. J Biol Chem 2004;279:47109–14. [PubMed: 15377660]

Ye J, Rawson RB, Komuro R, Chen X, Dave UP, Prywes R, Brown MS, Goldstein JL. ER stress induces cleavage of membrane-bound ATF6 by the same proteases that process SREBPs. Mol Cell 2000;6:1355–64. [PubMed: 11163209]

Yoshida H, Oku M, Suzuki M, Mori K. pXBP1(U) encoded in XBP1 pre-mRNA negatively regulates unfolded protein response activator pXBP1(S) in mammalian ER stress response. J Cell Biol 2006;172:565–75. [PubMed: 16461360]

Zhang P, McGrath B, Li S, Frank A, Zambito F, Reinert J, Gannon M, Ma K, McNaughton K, Cavener DR. The PERK eukaryotic initiation factor 2 alpha kinase is required for the development of the skeletal system, postnatal growth, and the function and viability of the pancreas. Mol Cell Biol 2002;22:3864–74. [PubMed: 11997520]

NIH-PA Author Manuscript
NIH-PA Author Manuscript
NIH-PA Author Manuscript

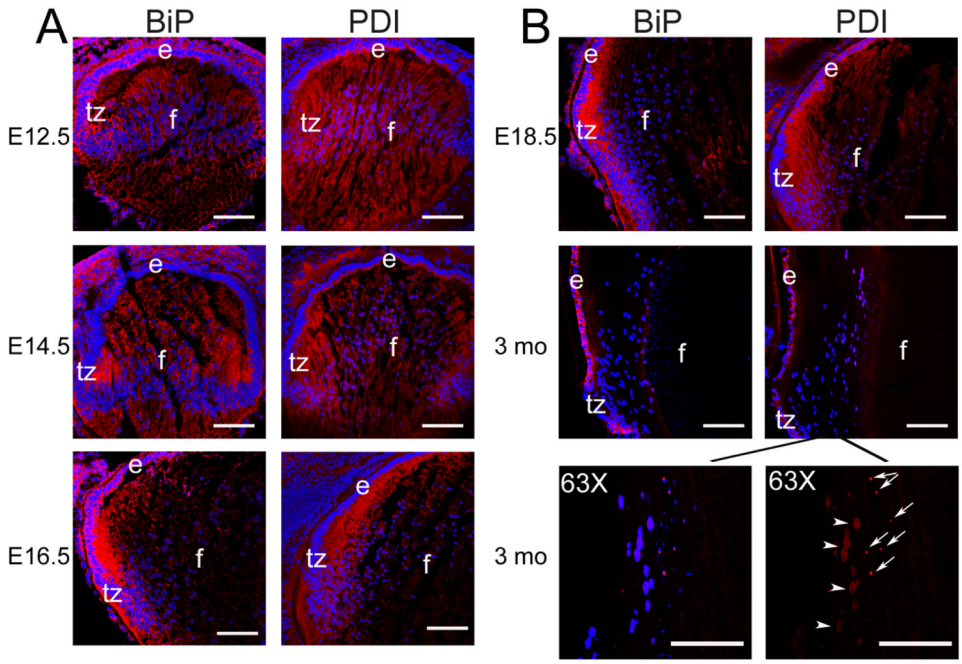

Figure 1. Expression of ER chaperones BiP and PDI in embryonic and adult mouse lenses

Expression of BiP and PDI in WT lenses detected by immunofluorescence. A) At E12.5, both ER chaperones are expressed throughout primary lens fiber cells and lens epithelium (top panels). At E14.5, the expression of BiP and PDI is elevated at the transition zone compared to the central fibers (middle panels) and by E16.5 it becomes mostly confined to the newly forming fiber cells (bottom panels). B) At E18.5, while the expression of both ER chaperones is still high in the newly forming lens fiber cells and lens epithelium, there is only a diffuse staining in central lens fiber cells (top panels). In 3 month old lenses, BiP and PDI expressions are now associated with fiber cells that are getting ready to undergo degradation of nuclei and organelles (middle panels). Bottom panels show higher magnification images of PDI expression in fiber cells. Perinuclear staining in fiber cells that are getting ready to undergo denucleation (white arrow heads) and a dot-like staining at the tips of degrading nuclei (white arrows). Bars, 100 m; e, epithelium; f, fiber cells; tz, transition zone. In all panels blue labels DNA, red labels BiP (left panels) or PDI (right panels).

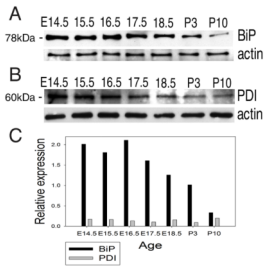

Figure 2. Immunoblot analysis of BiP and PDI expression

A) The major ER chaperone BiP is highly expressed in embryonic lenses. B) Another ER chaperone PDI is also expressed in the lens throughout development; although at lower amounts compared to BiP. Actin was used as a loading control. C) The intensity of the signal on the blots was calculated using Photoshop Histogram Analysis. Relative expression of BiP and PDI normalized to actin is plotted as bar graphs.

NIH-PA Author Manuscript NIH-PA Author Manuscript NIH-PA Author Manuscript

NIH-PA Author Manuscript
NIH-PA Author Manuscript
NIH-PA Author Manuscript

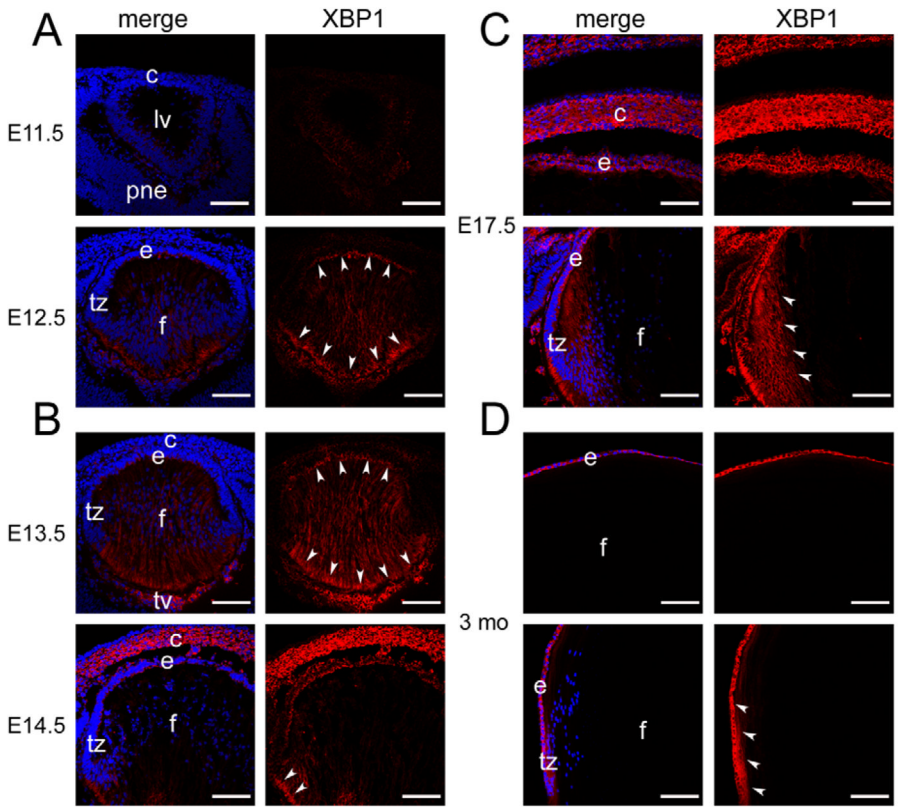

Figure 3. Expression of XBP1 in embryonic and adult lenses

Expression of XBP1 (both spliced and unspliced) in WT lenses detected by immunofluorescence. A) At E11.5, there is no XBP1 expression detected in the lens vesicle (top panels). At E12.5, XBP1 expression becomes apparent throughout lens fiber cells, specifically at the apical and basal tips (bottom panels). B) At E13.5, XBP1 expression is still high throughout lens fiber cell cytoplasm and apical and basal tips (top panels). At E14.5, XBP1 downregulates in lens fiber cells while epithelial XBP1 expression increases (bottom panels). Arrowheads indicate the apical and basal tips of lens fiber cells. C) At E17.5, along with the cornea, lens epithelium shows high XBP1 expression (top panels) while in lens fiber cells, XBP1 expression is observed only in peripheral fiber cells (bottom panels). D) At 3 months, while lens epithelial XBP1 expression stays up (top panels), the expression of XBP1 in fibers is restricted only to the newly forming lens fiber cells (bottom panels). Arrowheads point the newly forming lens fiber cells that express XBP1. Bars, 100 m; c, cornea; e, epithelium; f, fiber cells; lv, lens vesicle; pne, proliferative retinal neuroepithelium; tz, transition zone. In all panels blue labels DNA, red labels XBP1.

NIH-PA Author Manuscript

NIH-PA Author Manuscript

NIH-PA Author Manuscript

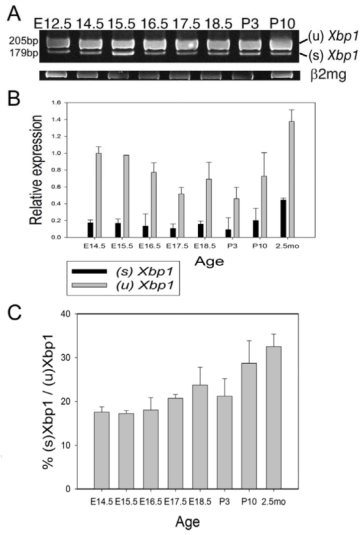

Figure 4. Conventional and real-time RT-PCR analysis of XBP1 splicing

A) Conventional RT-PCR analysis was performed to detect IRE1-induced *Xbp1* splicing. There is a basal level of *Xbp1* splicing throughout lens development. 2mg was used as a loading control. B) Real-time RT-PCR analysis was performed to quantify *Xbp1* expression. The relative expression of total and spliced *Xbp1* transcripts normalized to 2mg is plotted as bar graphs. The expression of total *Xbp1* at E14.5 is set to 1. C) The bar graph represents the ratio of spliced *Xbp1* transcripts to total *Xbp1* transcripts during lens development. The spliced *Xbp1* transcript represents about %17 of total *Xbp1* transcripts at E14.5 and about %32 of total *Xbp1* transcripts at 2.5 months.

NIH-PA Author Manuscript

NIH-PA Author Manuscript

NIH-PA Author Manuscript

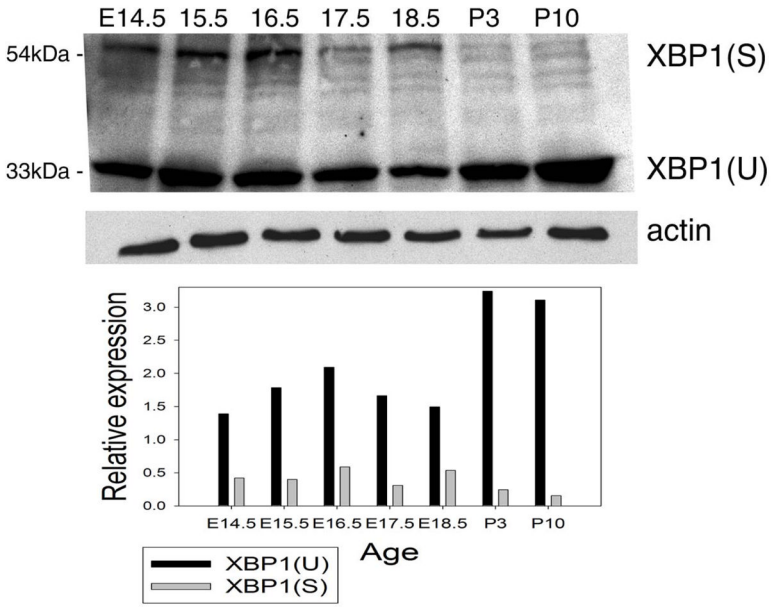

Figure 5. Immunoblot analysis of XBP1 expression

XBP1(S) protein translated from spliced *Xbp1* transcript is found at high levels in embryonic lenses, whereas in postnatal lenses, this protein is not at detectable levels. XBP1(U) protein produced from the unspliced *Xbp1* transcript is found at high levels throughout lens development and upregulates postnatally. Actin was used as a loading control. The intensity of the signal on the blots was calculated using Photoshop Histogram Analysis. Relative expression of XBP1(S) and XBP1(U) normalized to actin is plotted as bar graphs.

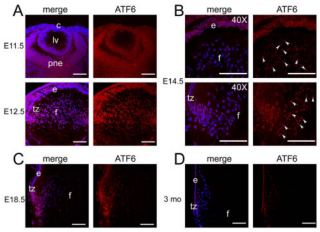

Figure 6. ATF6 expression in embryonic and adult mouse lenses

Expression of ATF6 (both full length and cleaved) in WT lenses detected by immunofluorescence. A) At E11.5, there are low amounts of ATF6 expression in the posterior lens vesicle cells and the retina (top panels). At E12.5, ATF6 expression is detected at high levels in the fiber cell nuclei (bottom panels). B) At E14.5, there are low amounts of ATF6 expression in the lens epithelium (top panels), while ATF6 is highly expressed by lens fiber cells (bottom panels). Arrowheads indicate the nuclei of lens fiber cells that express ATF6. C) At E18.5, the expression of ATF6 is highest at the transition zone where the newly forming fiber cells are found. D) In 3 month old lenses, ATF6 expression is still detectable in lens epithelium and fiber cells. Bars, 100 m; c, cornea; e, epithelium; f, fiber cells; lv, lens vesicle; pne, proliferative retinal neuroepithelium; tz, transition zone. In all panels blue labels DNA, red labels ATF6.

NIH-PA Author Manuscript NIH-PA Author Manuscript NIH-PA Author Manuscript

NIH-PA Author Manuscript

NIH-PA Author Manuscript

NIH-PA Author Manuscript

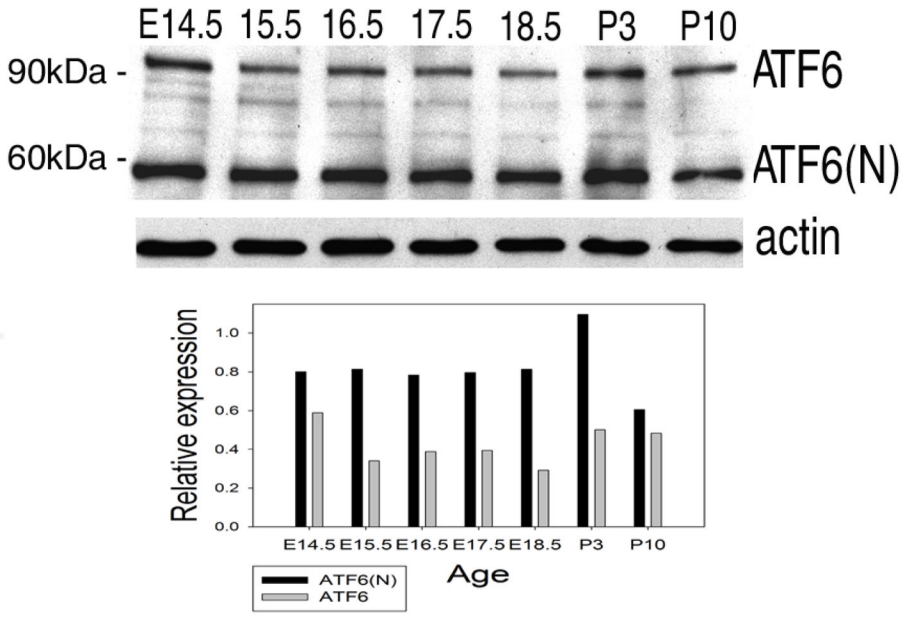

Figure 7. Immunoblot analysis of ATF6 cleavage

ATF6 protein is cleaved into its nuclear form (ATF6(N)) upon activation. In both embryonic and postnatal normal lenses, ATF6(N) is present. Actin was used as a loading control. The intensity of the signal on the blots was calculated using Photoshop Histogram Analysis. Relative expression of ATF6 and ATF6(N) normalized to actin is plotted as bar graphs.

NIH-PA Author Manuscript

NIH-PA Author Manuscript

NIH-PA Author Manuscript

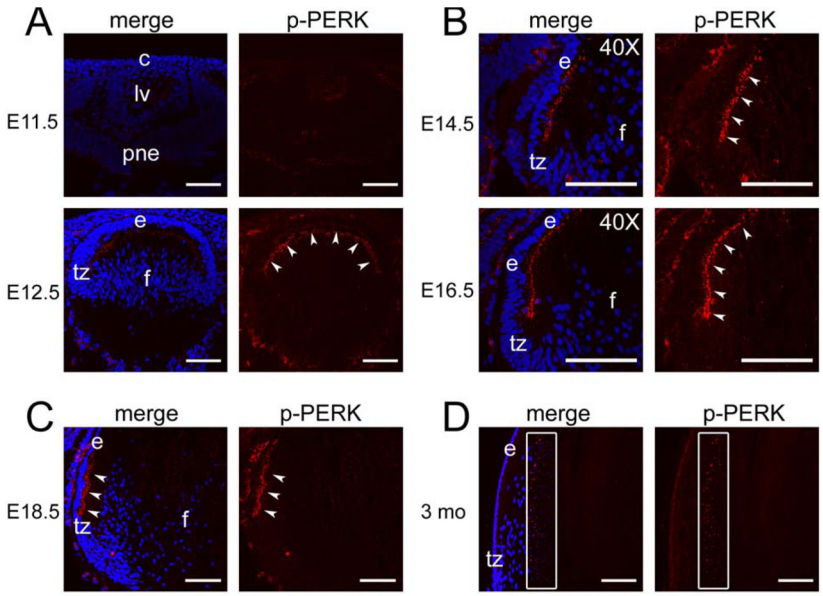

Figure 8. Expression of p-PERK in embryonic and adult lenses

Expression of p-PERK in WT lenses detected by immunofluorescence. A) At E11.5, there is no p-PERK expression detected in the lens vesicle (top panels). At E12.5, p-PERK expression becomes apparent at the apical tips of lens fiber cells (bottom panels). B) In E14.5 and E16.5 lenses, p-PERK expression is still high at the apical tips of lens fiber cells, specifically at the apical tips of newly forming lens fiber cells. C) At E18.5, p-PERK expression is confined to the peripheral fiber cells. Arrowheads indicate the apical tips of lens fiber cells. D) In 3 months old lenses, p-PERK is expressed by lens fiber cells that are degrading their nuclei. The boxed area indicates the region where p-PERK is expressed. Bars, 100 m; c, cornea; e, epithelium; f, fiber cells; lv, lens vesicle; pne, proliferative retinal neuroepithelium; tz, transition zone. In all panels blue labels DNA, red labels p-PERK.

NIH-PA Author Manuscript
NIH-PA Author Manuscript
NIH-PA Author Manuscript

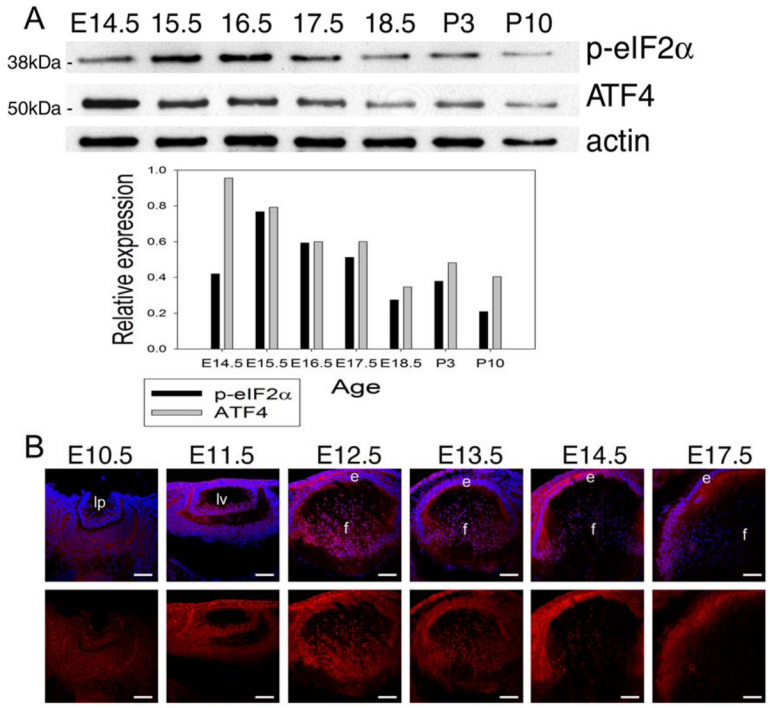

Figure 9. Expression of ATF4 and p-eIF2 during lens development

A) Western blotting analysis was performed to detect phospho eIF2 (p-eIF2) and ATF4 levels. The levels of p-eIF2 increase around E15.5–E16.5 and downregulate postnatally. Similarly, ATF4 levels are high in embryonic lenses (E14.5–E16.5); however downregulate in postnatal lenses. Actin was used as a loading control. The intensity of the signal on the blots was calculated using Photoshop Histogram Analysis. Relative expression of XBP1(S) and XBP1(U) normalized to actin is plotted as bar graphs. B) Expression of ATF4 in WT lenses detected by immunofluorescence. ATF4 expression is high at E12.5 lens fiber cells but downregulate after E14.5. Bars, 77 m; c, cornea; e, epithelium; f, fiber cells; lv, lens vesicle; tz, transition zone. In all panels blue labels DNA, red labels ATF4.

NIH-PA Author Manuscript

NIH-PA Author Manuscript

NIH-PA Author Manuscript

Table 1

Antibodies used in this study

Antibody		**IF**	**WB**
Rabbit polyclonal to BiP	Abcam (Cambridge, MA)	1:400	1:1000
Rabbit polyclonal to PDI	Abcam (Cambridge, MA)	1:200	1:1000
Rabbit polyclonal to total-Xbp1	Santa Cruz Biotechnolog Inc., (Santa Cruz, CA)	1:200	1:1000
Rabbit polyclonal to ATF6	ProSci Inc. (Poway, CA)	1:200	1:1000
Rabbit polyclonal to phospho-PERK	Cell Signaling Technology Inc. (Danvers, MA)	1:200	-
Rabbit polyclonal to phospho-eIF2	Invitrogen (Carlsbad, CA)	-	1:1000
Rabbit polyclonal to ATF4/CREB2	Santa Cruz Biotechnology Inc., (Santa Cruz, CA)	1:200	1:1000
Rabbit polyclonal to actin	Sigma-Aldrich, St. Louis, MO	-	1:3000